AQUEOUS SODIUM PHOSPHATE HIDEOUT REACTIONS WITH NICKEL AND TITANIUM OXIDES UNDER CANDU-PHW BOILER CONDITIONS.

M. Madekufamba: M.Sc Student

L. Trevani; P. Tremaine: Supervisors

Department of Chemistry, University of Guelph, Guelph, Ontario. Canada N1G 2W1

Phosphate methods of chemistry control are widely used in thermal power stations and less widely in nuclear stations because of concerns about metal-phosphate "hideout" reactions. In this work, nickel phosphate and titanium phosphate hideout products that can form under CANDU-PHW reactor conditions have been synthesized using hydrothermal methods. The pure crystalline solids that were obtained have been characterised by Raman spectroscopy, ICP and FTIR and XRD. Two different solid phases were obtained from the synthesis with nickel oxide while one solid phase was obtained from titanium oxide. Solubility studies were carried out for the sodium titanium phosphate product. The results were used to derive thermodynamic models for the interaction of metal oxides with high temperature aqueous sodium phosphates. The thermochemical constants for the hideout reaction products are consistent with the geochemical thermodynamic database SUPCRT92 and other data bases used to model corrosion product behaviour.

1 INTRODUCTION

Most North American thermal electric power stations use boiler-water pH control strategies base on millimolar additions of sodium phosphate, the so-called "Equilibrium" and "Coordinated" Phosphate Treatments. Phosphate methods are much less widely used in nuclear stations because of concerns about metal-phosphate "hideout" reactions which may take place at high temperatures and pressure if local, under-deposit chemistry conditions cause metal oxides to react with aqueous sodium phosphate [1-3]. This experience led to some power plants including the Point Lepreau NGS to change over from phosphate treatments to ‘All-Volatile Treatment’ control.

CANDU boiler tubes are fabricated from Incoloy 800, and titanium is becoming more widely used as a material in low-temperature heat exchangers and condensers. The purpose of this project was to identify the nickel and titanium oxide reaction products that would form under CANDU-PHW reactor conditions, to synthesize pure samples of these compounds, and to measure the solubility of the reactor products from the titanium oxide in sodium phosphate solutions under boiler conditions. The solubility data and structural properties were then used to derive a chemical equilibrium model for the hideout reactions that is compatible with databases used for modelling corrosion product behaviour.

2. MATERIALS AND EXPERIMENTAL PROCEDURES

2.1 Synthesis of $Na_2Ni_{0.8}(OH)_{0.32}PO_4(s)$ and $Na_4Ti(OH)_2(PO_4)_2(s)$.

Nickel and titanium hideout products were synthesized by reacting the corresponding oxide NiO(s) or TiO_2(s, rutile) with aqueous sodium phosphate at 200 °C and 250 °C. Reactions were carried out in modified Parr digestion vessels. The vessels were equipped with Teflon liners and platinum filters. The experiments were allowed to proceed for at least 10 days. The experimental design [2] allowed reaction products to be separated from the aqueous phase before the vessel was cooled down to room temperature.

Characterization of the reaction products was done using (i) powder X-ray diffraction (Rigaku Geigerflex Dmax II X-ray difractometer with a cobalt source and a graphite crystal monochrometer), (ii) Raman spectroscopy (Renishaw Raman Imaging Microscope System 2000 with argon ion laser at 514 nm), (iii) Scanning electron microscopy (Hitachi S-4500 Field Emission SEM with Quartz-X-One X-ray microanalysis system). Chemical compositions were determined by ICP-ES elemental analysis.

2.2 Solubility of TiO_2(s) in sodium phosphate solutions

Reactions were carried out in a 450 mL zirconium Parr stirred pressure vessel (Model 4562) with a proportional integral derivative (PID) temperature controller and pressure display unit. Kinetic experiments were carried out at 250 °C to determine the time required to reach equilibrium. Temperature-dependent solubility measurements were carried out from 240 °C to 300 °C. Experiments were designed to maintain an excess amount of the metal oxide in the pressure vessel. The temperature was raised to a desired value and the reaction was allowed to proceed at this temperature while the reaction product was formed until equilibrium was established between the two solids. By ensuring that there is an excess of both solid reactant and product, there is no need to determine the amounts of solid in the vessel as chemical equilibrium will only depend on aqueous species. The first set of temperature dependent studies were carried out by increasing the temperature in incremental stages and taking solution samples at each temperature up to a maximum of 300 °C. After that, experiments were repeated by starting at high temperature then decreasing temperature and taking solution samples after allowing equilibration time at each temperature. Samples collected from the solubility vessel were analyzed by ICP-ES for total phosphate and sodium molality.

3. HYDROTHERMAL SYNTHESIS RESULTS

3.1 Characterisation of the Nickel Reaction Product

The major hideout reaction product was found to be sodium nickel hydroxyphosphate $Na_2Ni_{0.8}(OH)_{0.32}PO_4(s)$ (SNHP)[4] based on ICP-ES data. The powder XRD pattern as well as the scanning electron micrograph of the bright green crystals of the solid are shown in Figure 1.The FTIR and Raman spectra of SNHP are shown in Figures 2 and 3 respectively.

The presence of the hydroxyl group in the structure of SNHP is confirmed in the FTIR (Figure 2) by the O–H stretching band at 3500 cm^{-1}. The Raman spectrum shows the P–O stretching bands at (900-1100 cm^{-1}) and the O– P-O bending modes (600 to 400 cm^{-1}). At higher phosphate concentration and Na/P ratios > 2.5 a solid solution of cubic trisodium phosphate $Na_{(3-2x)}Ni_xPO_4(s)$ is also formed. Figure 4 shows powder XRD and SEM image of the cubic phosphate $Na_{2.6}Ni_{0.2}PO_4$.

3.2 **Characterisation of titanium reaction product**

The major hideout product was found to be $Na_4Ti(OH)_2(PO_4)_2$ [5] and a minor non-stoichiometric product $Na_2Ti_{0.6}(OH)_{1.4}(PO_4)$. The powder XRD pattern of sodium titanium hydroxyphosphate (STHP), $Na_4Ti(OH)_2(PO_4)_2$ and its SEM image are shown in Figure 5. The crystals of STHP are white and transluscent under the microscope. Figure 6 is its Raman spectrum with the characteristic P-O stretching modes(900-1100 cm^{-1}) and O-P-O bending modes (400-600 cm^{-1}). The FTIR spectrum for STHP showed a small O-H stretching band at 3450 cm^{-1} confirming the existence of hydroxyl group in the structure of STHP, Figure 7.

4.0 SOLUBILITY RESULTS

4.1. **Solubility of TiO_2(s)**

Experiments were carried out in the same way as the NiO(s) system above and the results were analysed assuming the reaction:

$$TiO_2(s) + 4Na^+(aq) + 2HPO_4^{2-}(aq) \rightleftharpoons Na_4Ti(OH)_2(PO_4)_2(s). \qquad (1)$$

Kinetic experiments showed that 48 hours is required for the reaction to reach equilibrium. All samples in the solubility experiments were collected after 48 hours at the temperature under investigation. The total phosphate and Na^+ in the solutions were measured by ICP-ES and used with the computer program MULTEQ to calculate the equilibrium constant at different temperatures according to equation 2 .

$$K = Q/\{[\gamma_{Na+}]^4[\gamma_{HPO4}{}^{2-}]^2\} \qquad (2)$$

where Q is the concentration quotient and γ is the activity coefficient for the aqueous species. The corresponding Gibbs energies were calculated from the expression:

$$\Delta_r G_T{}^o \;=\; -RT\;\ln K \qquad (3)$$

Apparent Gibbs free energies of the species in equation 1 were obtained from computer programme SUPCRT92 and used together with Gibbs energies from equation 3, to calculate apparent Gibbs energies of formation of STHP, $\Delta_a G_f{}^o$(STHP,s). Calculated values were fitted to equation 4 which shows variation of Gibbs energies with temperature. The Maier-Kelly heat capacity function was derived from experimental heat capacities of STHP and the pressure effect was assumed to be negligible in equation 4.

$$\Delta_a G^o{}_T = \Delta_f G^o{}_{298}\,(T - 298.15) - S^o{}_{298}\,(T - 298.15) + a\,(T - 298.15) + (d/2)\,(T^2 - 298.15^2) -$$

$$c\,(1/T - 1/298.15) - T\;[\,a\ln(T/298.15) + b\,(T - 298.15) + (c/2)\,(1/T^2 - 1/298.15^2)] +$$

$$V^o{}_{298}(P - 0.1) \qquad (4)$$

Figure 8 shows the apparent Gibbs energies of formation of STHP, $\Delta_a G_f{}^o$(STHP,s) as a function of temperature together with a fit of equation 4. The fitted parameter gave values for the standard Gibbs energy for STHP, $\Delta_f G^o$(STHP,s) = -4138.6 ± 7.0 kJ·mol^{-1} and standard entropy of STHP. S^o(STHP,s) = 294 ± 42 J·K·mol^{-1}. These were used to calculate a value for the standard enthalpy of STHP as $\Delta_f H^o$(STHP,s) = -4476.3 ± 8.4 kJ·mol^{-1}.

5. CONCLUSIONS

The possible hideout reaction products that can form from nickel oxide and titanium oxide interactions with sodium phosphate under boiler conditions were identified. Thermodynamic data for the hideout products were obtained and these are a significant contribution to thermodynamic databases. Thermodynamic models were derived for the interaction of the metal oxides with sodium phosphates under CANDU boiler conditions.

REFERENCES

[1] Tremaine P. R., Schvedov D., Trevani L and Xiao C. Sodium Phosphate Hideout Mechanisms, *EPRI Report* **TR-112137** (1999)
[2] Bridson J. N., Quinlan S and Tremaine P.R. *Chem.Mater* **10(3)** 763-768 (1998)
[3] Alexander J. H and Luu L. MULTEQ Code, Vol 1 Uses Manual. *EPRI Report* **NP-5561** (1992).
[4] Ziemniak S. E and Opalka E. P Proceedings of the International Symposium on Environmental Degradation of Materials in Nuclear Power Systems-Water Reactors, **153** 153-156 (1988)
[5] Ziemniak S. E., and Opalka E. P. *Chem.Mater* **5** 690-694 (1993).
[6] Johnson J. W., Oelkers E. H and Helgeson H. C. SUPCRT92: *Computers and Geoscience* **18(7)** 1991.

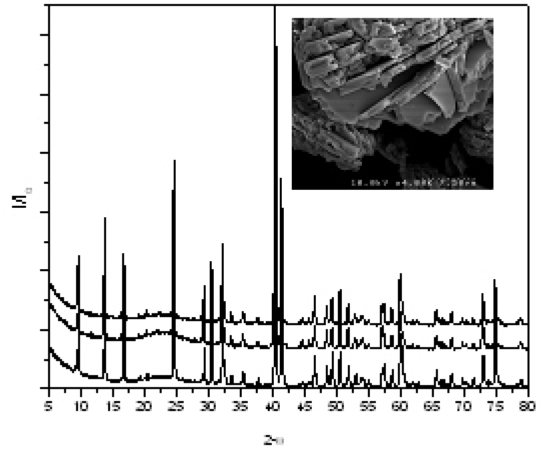

Figure 1: Powder XRD pattern and SEM image for $Na_2Ni_{0.8}(OH)_{0.32}PO_4(s)$

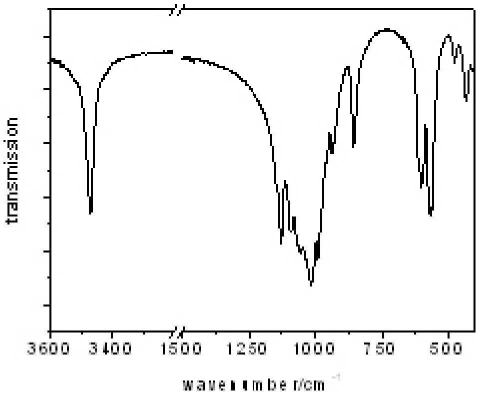

Figure 2: FTIR spectrum for $Na_2Ni_{0.8}(OH)_{0.32}PO_4(s)$

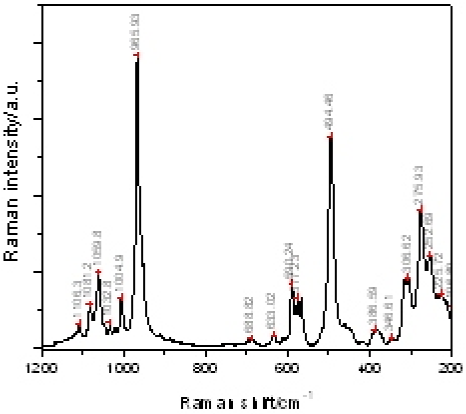

Figure 3: Raman spectrum $Na_2Ni_{0.8}(OH)_{0.32}PO_4(s)$

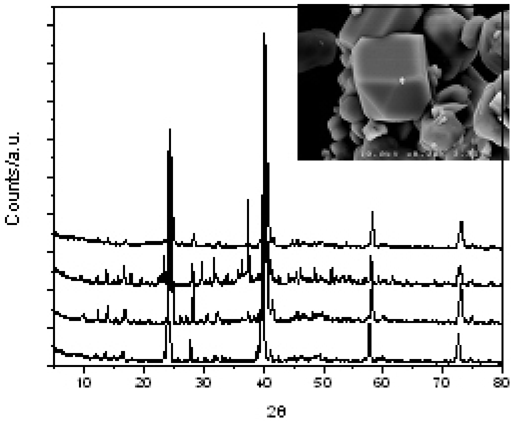

Figure 4: Powder XRD pattern and SEM images for $Na_{2.6}Ni_{0.2}PO_4(s)$

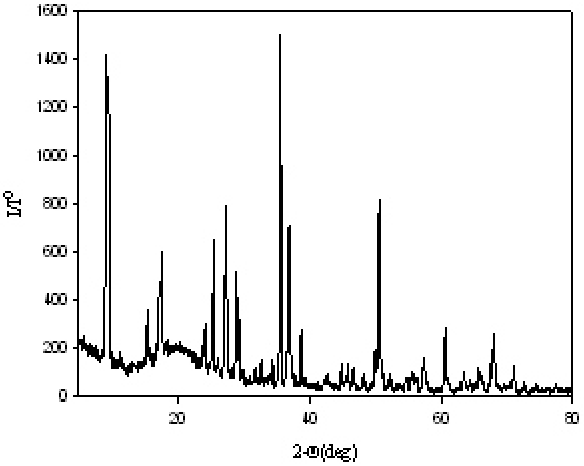

Figure 5: Powder XRD pattern of STHP

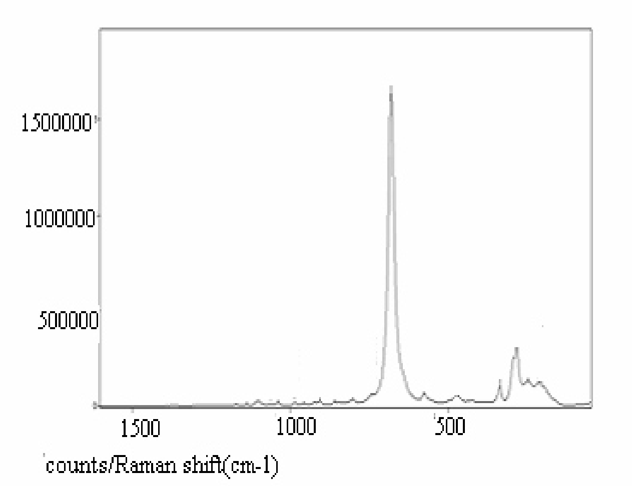

Figure 6: Raman spectrum of STHP

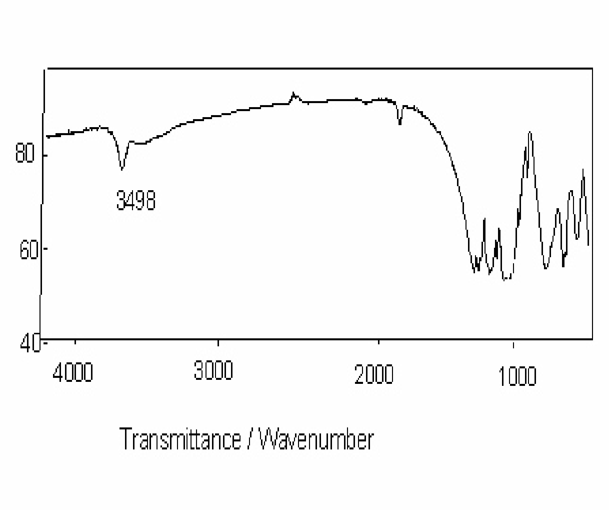

Figure7: FTIR spectrum for STHP(s)

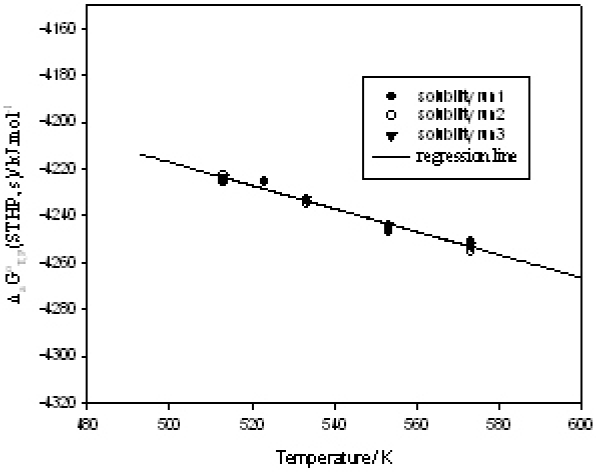

Figure 8: Regression of experimental apparent Gibbs free energy of formation of STHP with equation 4.